

On-Demand Trajectory Predictions For Interaction Aware Highway Driving

Cyrus Anderson¹, Ram Vasudevan², and Matthew Johnson-Roberson³

Abstract—Highway driving places significant demands on human drivers and autonomous vehicles (AVs) alike due to high speeds and the complex interactions in dense traffic. Merging onto the highway poses additional challenges by limiting the amount of time available for decision-making. Predicting others' trajectories accurately and quickly is crucial to safely executing these maneuvers. Many existing prediction methods based on neural networks have focused on modeling interactions to achieve better accuracy while assuming the existence of observation windows over 3 s long. This paper proposes a novel probabilistic model for trajectory prediction that performs competitively with as little as 400 ms of observations. The proposed method fits a low-dimensional car-following model to observed behavior and introduces nonconvex regularization terms that enforce realistic driving behaviors in the predictions. The resulting inference procedure allows for realtime forecasts up to 10 s into the future while accounting for interactions between vehicles. Experiments on dense traffic in the NGSIM dataset demonstrate that the proposed method achieves state-of-the-art performance with both highly constrained and more traditional observation windows.

Index Terms—Autonomous Vehicle Navigation, Autonomous Agents

I. INTRODUCTION

This work focuses on predicting vehicles' future trajectories for enabling autonomous vehicles (AVs) to merge onto highways. Merging necessitates cooperating with other drivers, and predicting others' actions is crucial to successful cooperation. Predicting a vehicle's trajectory, however, is complicated by its possible interactions with surrounding vehicles [1], [2]. Recent works based on deep neural networks have proven effective at modeling these interactions [3]–[7]. These methods utilize a fixed number of observations of surrounding vehicles to infer which trajectories are likely. A drawback to this is the duration of time needed to collect observations before making predictions, ranging from 3 s up to 5 s. While limited ramp length limits the time available to complete a merge, the long observation windows used in these methods further restricts the time available to make decisions. Sensor limitations such as maximum range and occlusions also impact the quality of any observations of the surrounding vehicles. This motivates the need for predictions that can be made in short time and with few observations. Here we aim to strike a balance between the richness of interactions modeled and the number of observations needed to make predictions.

This work was supported by a grant from Ford Motor Company via the Ford-UM Alliance under award N022884.

¹C. Anderson is with the Robotics Institute, University of Michigan, Ann Arbor, MI 48109 USA andersct@umich.edu

²M. Johnson-Roberson is with the Department of Naval Architecture and Marine Engineering, University of Michigan, Ann Arbor, MI 48109 USA mattjr@umich.edu

³R. Vasudevan is with the Department of Mechanical Engineering, University of Michigan, Ann Arbor, MI 48109 USA ramv@umich.edu

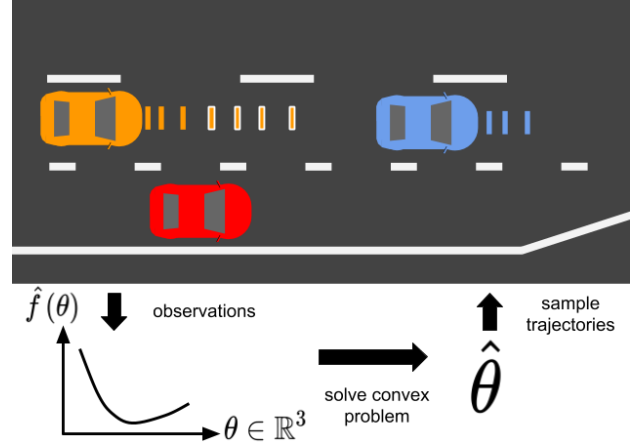


Figure 1: Overview of prediction method. The autonomous vehicle (red) seeks to predict the trajectories of the front and rear (lead and lag) vehicles to enable a safe merge between them. Observations of both vehicles over a short time (orange and blue marks) are used to define a likelihood function over possible controllers θ for the lag vehicle. Solving a convex problem yields an estimate that is used to sample realistic trajectories (orange highlighted marks).

This work presents a novel method to predict vehicle trajectories in ramp merge scenarios, with as little as 400 ms of observations. We use the car-following model proposed by Wei et. al. [8] to predict trajectories. This is done by treating the parameters of the model as unknown and solving the resulting estimation problem. In our probabilistic framework we use the observations of the lead and lag vehicles depicted in Figure 1 along with a data-dependent prior to obtain an initial estimate of the unknown parameters. Though the original estimation problem is nonconvex, we convert it to a semidefinite program that can be solved quickly. To improve the estimate robustness we then apply a nonconvex regularization term when sampling trajectories. Our main contributions are:

- 1) a novel probabilistic highway interaction model utilizing a nonconvex regularization term;
- 2) a realtime and consistent inference procedure;
- 3) evaluation on the real-world NGSIM dense highway traffic dataset [9].

The paper is organized as follows. Section II describes related works in interaction-based trajectory prediction for traffic participants in general scenarios and those focused on ramp merging. Section III describes the interaction model we use to make predictions and the inference procedure used to determine the probabilities of different outcomes. We evaluate our model on the NGSIM dataset and perform an ablation

study in Section IV before concluding in Section V.

II. RELATED WORK

We first describe prediction methods that may operate on highly restricted observation windows, but do not take into account interactions. Methods that focus on modeling interactions, but operate on longer observation windows, are described in the next section. In the last section we describe methods designed specifically to account for the interactions and restricted observation windows in ramp merging scenarios.

A. Single Agent Prediction

Classical methods specify a simple kinematic model to predict trajectories, such as constant velocity or constant yaw rate and acceleration (CYRA). Other methods have employed learning based approaches to learn a representation of likely trajectories given observations such as [10], which uses Gaussian mixture models to represent the future trajectory, or [11], which uses a hidden Markov model over simple kinematic models. The CYRA model is combined with a maneuver prediction module to better account for long-term motion in [12]. They select trajectories to predict using a penalty on future accelerations similar to the one proposed here. These methods, however, do not account for interactions between different vehicles on the road. This can lead to inconsistent predictions in common scenarios such as a fast vehicle needing to slow down for a vehicle in front.

B. General Interaction-Based Trajectory Prediction

More recent works have leveraged observations of surrounding vehicles to make more accurate predictions. Many of these are based on neural networks. In [3] the trajectory prediction takes the form of occupancy grids at the future times. The predictions produce a distribution over occupancy, but the occupancy grids do not preserve the label of which vehicle occupies which position. A two-stage approach is employed in [4] wherein a first LSTM predicts the given vehicle's lane change intent, and this prediction is then input to a second LSTM that separately predicts the future lateral deviations and longitudinal accelerations. Though [4] does not produce probabilistic predictions, the works [5]–[7] do so by predicting bivariate Gaussian distributions. The probabilistic methods of [5], [6] make use of highway structure and assign a confidence to each type of specified maneuver. For each maneuver another neural network predicts the vehicle's trajectory. The neural network proposed in [7] is designed for use in non-highway driving as well so it uses the observations of each road user's state directly without specifying maneuvers. In this work we focus only on predicting trajectories for ramp merge scenarios, particularly those where the vehicles do not merge into different lanes. The proposed method can thus be seen as the predictor for a specific maneuver, the one that leads to the more difficult scenario of needing to merge into a more crowded space. Another difference in usability between the proposed method and the neural networks is the duration of the observation window and forecast horizon. The

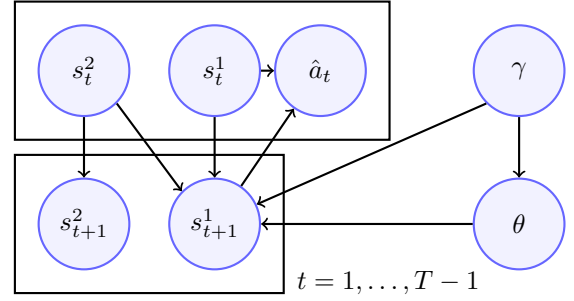


Figure 2: Proposed interaction model for predicting lag vehicle behavior. The lag vehicle state s^1 depends on the lead vehicle's state s^2 , its own controller θ , and hyperparameters γ .

proposed method can observe as little as 400 ms and forecast competitively to 10 s, whereas the other methods use 3 s–5 s for observation before a forecast of up to 5 s. A lengthy observation window may not be available in difficult scenarios calling for rapid decisions.

Other works not based on neural networks have manually defined cost functions that specify vehicles' behavior as in [13]. The cost function proposed in [14] is based on Hidden Markov Models learned from real data, and an integer linear program is solved to predict likely trajectories. These methods, however, have not performed as well as those based on neural networks.

C. Ramp Merging Trajectory Prediction

A number of works focus on predicting trajectories to enable safer ramp merging. For this they predict the trajectory of the vehicle (lag vehicle) in front of which the ego vehicle may merge. In [15] the lag vehicle dynamics are modeled as a Markov chain. One Markov chain is learned for each case of the lag vehicle yielding, and not yielding, to the merging vehicle. As the yielding intent is unknown, the two models are ensembled to make predictions. A similar approach by [16] uses the Intelligent Driver Model (IDM) [17] instead of the Markov chain. The parameters for each yielding intent's IDM are manually chosen. The proportional controller in this work used for prediction was proposed in [8] where its gain and setpoint parameters were not based on observations. In this work we treat the parameters as unknown and predict the trajectories of controllers corresponding to likely parameters. Compared to [15], [16], which both predict using an ensemble of finitely many models, this work uses infinitely many. This is a result of accounting for uncertainty in our parameters over a continuous space. The same can be said for simple kinematic models such as the constant velocity model with uncertainty, but our models account for interactions.

III. ON-DEMAND TRAJECTORY PREDICTIONS

We aim to make trajectory predictions for the ramp merging scenario that take into account observed interactions, in addition to requiring only a minimal number of observations. Section III-A states the trajectory prediction problem in our

probabilistic setting. Section III-B defines the interaction-based controller whose parameters we aim to estimate, and the dynamics of the system. The full probabilistic model with novel nonconvex regularization terms is defined in Section III-C. The realtime inference procedure for predicting trajectories with this model is described in Section III-D.

A. Problem Statement

We consider the ramp merging scenario in Figure 1 depicting the AV merging onto the highway. To enable safe merging we are interested in predicting the longitudinal positions of the two (lead, lag) vehicles in the target lane. Let $s_t^i = (x_t^i, v_t^i)^\top$ denote the state of vehicle i consisting of position $x_t^i \in \mathbb{R}$ and velocity $v_t^i \in \mathbb{R}$ at timestep t . We denote the state of the lag vehicle by s_t^1 and state of the lead vehicle by s_t^2 . We observe the state of both vehicles $s_t = (s_t^1, s_t^2)^\top$ at timesteps $t = 1, \dots, k$ and predict x_t^1 until the final timestep, $t = k+1, \dots, T$. Additionally we will use the subscript notation $i : j$ to refer to the set of variables indexed by $i, i+1, \dots, j$. In making probabilistic predictions this amounts to sampling

$$x_{k+1:T}^1 \sim p(x_{k+1:T}^1 | s_{1:k}). \quad (1)$$

We now explain our focus on the lag vehicle. With several assumptions summarized in the graphical model shown in Figure 2, we decompose the joint prediction of both vehicles into two parts. The first part predicts the lead vehicle's trajectory and the second predicts the lag vehicle's trajectory conditioned on that of the lead vehicle.

We start with the assumption of not having observations for the vehicle in front of the lead vehicle. We model the lag vehicle behavior as dependent on the state of the lead vehicle, yet we do not model the state of the lead vehicle as dependent on its own lead. One reason for this inconsistency is that occlusions and limited sensor range may prevent us from obtaining such observations. Aside from this, the proposed model could be extended to account for the lead vehicle's own lead by repeated decomposition, but there is a point at which we cannot see further vehicles ahead. We thus present the simplest model here. Next assume that the lead vehicle's actions do not depend on the lag vehicle's state as in common car-following models. Furthermore assume the measurements of position and velocity are noiseless, while the acceleration measurement \hat{a}_t has Gaussian noise with a small variance σ_a^2 . This is reasonable when the former measurements have low variances but acceleration is approximated from velocity via finite differences. Given velocity measurements with variance σ_v^2 and timestep size Δt , acceleration then has variance $\text{var}(\hat{a}_t) = \text{var}(v_{t+1} - v_t) / \Delta t^2 = 2\sigma_v^2 / \Delta t^2$. The small timestep will magnify the variance as in the NGSIM dataset.

Using the independence assumptions in graphical model shown in Figure 2 we may write

$$\begin{aligned} & p(s_{k+1:T} | s_{1:k}) \\ &= p(s_{k+1:T}^1 | s_{1:k}, s_{k+1:T}^2) p(s_{k+1:T}^2 | s_{1:k}) \\ &= p(s_{k+1:T}^1 | s_{1:k}, s_{k+1:T}^2) p(s_{k+1:T}^2 | s_{1:k}) \end{aligned} \quad (2)$$

which provides the problem decomposition. Throughout the remainder of this paper we focus on the prediction problem for the lag vehicle posed as

$$s_{k+1:T}^1 \sim p(s_{k+1:T}^1 | s_{1:k}, s_{k+1:T}^2) \quad (3)$$

from which we easily obtain the predicted positions.

B. Interaction Model

Here we describe the controller used to model the interactions between the lead and lag vehicle. The controller is based on balancing two goals. The first is to match the speed of the lead vehicle, and the second is to maintain a desired gap to the lead vehicle. Let g_t denote the current gap between the lead and lag vehicles. This gap is calculated from their positions as $g_t = x_t^2 - x_t^1 - l$, where l is the length of the lead vehicle. We denote the desired gap by g_* . Denoting k_v and k_g as the proportional terms for the desired speed and desired gap, respectively, we denote the parameters that define this controller by $\theta = (k_v, k_g, g_*)$. The controller proposed in [8] sets the lag vehicle's acceleration with

$$h(s_t, \theta) = k_v(v_t^2 - v_t) + k_g(g_t - g_*). \quad (4)$$

We assume that the proportional terms are bounded above by a constant \bar{k} and that each term is nonnegative. The space of possible parameters is thus equal to $[0, \bar{k}]^2 \times \mathbb{R}_+$, which we denote by Θ . We will use the notation $0_{m \times n}$ to denote the matrix of zeros with m rows and n columns. Given current state of the lag vehicle and controller parameters θ the next state is given by

$$s_{t+1}^1 = C s_t^1 + \left(\frac{\Delta t^2}{2} \right) h(s_t, \theta), \quad (5)$$

where

$$C = \begin{pmatrix} 1 & \Delta t \\ 0 & 1 \end{pmatrix}. \quad (6)$$

Given the lead vehicle's states we write the entire system dynamics as

$$\begin{pmatrix} s_t \\ 1 \end{pmatrix} = \begin{pmatrix} A(\theta) \\ 0_{1 \times 4} \ 1 \end{pmatrix} \begin{pmatrix} s_{t-1} \\ 1 \end{pmatrix} + \begin{pmatrix} 0 \\ 0 \\ s_t^2 \\ 0 \end{pmatrix}, \quad (7)$$

where

$$A(\theta) = \begin{pmatrix} B \\ 0_{2 \times 5} \end{pmatrix}, \quad (8)$$

and

$$B = (C \ 0_{2 \times 3}) + \left(\frac{\Delta t^2}{2} \right) \begin{pmatrix} -k_g \\ -k_v \\ k_g \\ k_v \\ -k_g(l + g_*) \end{pmatrix}^\top. \quad (9)$$

C. Regularized Prediction

The difficulty in sampling trajectories in (3) stems from not knowing the lag vehicle's controller θ . This section describes our novel model that employs regularization terms to assign lower probability to controllers that would produce unrealistic behaviors. We let $\gamma \in \Gamma$ represent the vector of regularization terms, which is an unknown random variable in the full model. Approximating the random variable γ with a known point estimate $\hat{\gamma}$, we can express the distribution of trajectories in (3) as

$$\begin{aligned} & p(s_{k+1:T}^1 | s_{1:k}, s_{k+1:T}^2) \\ &= \int_{\Theta} \int_{\Gamma} p(s_{k+1:T}^1, \theta, \gamma | s_{1:k}, s_{k+1:T}^2) d\theta d\gamma \\ &\approx \int_{\Theta} p(s_{k+1:T}^1, \theta | s_{1:k}, s_{k+1:T}^2, \hat{\gamma}) d\theta \\ &= \int_{\Theta} p(s_{k+1:T}^1 | s_{1:k}, s_{k+1:T}^2, \theta, \hat{\gamma}) p(\theta | s_{1:k}, s_{k+1:T}^2, \hat{\gamma}) d\theta \\ &= \int_{\Theta} p(s_{k+1:T}^1 | s_{1:k}, s_{k+1:T}^2, \theta, \hat{\gamma}) p(\theta | s_{1:k}, \hat{\gamma}) d\theta, \end{aligned} \quad (10)$$

where the last inequality follows from the conditional independence expressed in Figure 2. We begin by defining the second term in (10) which can be written using Bayes' rule and calculating the accelerations derived from velocities as

$$p(\theta | s_{1:k}, \hat{\gamma}) \propto p(\hat{a}_{1:k-1}, s_{2:k} | s_1, \theta, \hat{\gamma}) p(\theta | s_1, \hat{\gamma}). \quad (11)$$

For the first term in (11) we impose a recursive structure independent of γ to mirror standard Markov chain structure as

$$p(\hat{a}_{1:k-1}, s_{2:k} | s_1, \theta, \hat{\gamma}) = \prod_{i=1}^{k-1} p(\hat{a}_i, s_{i+1} | s_i, \theta), \quad (12)$$

which combined with the system dynamics in (7) and the assumed Gaussian noise for acceleration yields

$$\begin{aligned} p(\hat{a}_{1:k-1}, s_{2:k} | s_1, \theta, \hat{\gamma}) &= \prod_{i=1}^{k-1} p(\hat{a}_i | h(s_i, \theta)) = \\ &= \prod_{i=1}^{k-1} \mathcal{N}(\hat{a}_i; h(s_i, \theta), \sigma_a^2). \end{aligned} \quad (13)$$

Using this term only, we could estimate θ that fit the observed data. One problem with the estimated parameters is an occasionally large and unrealistic estimate of g_* . For this we define the second term in (11) as

$$-\log p(\theta | s_1, \hat{\gamma}) = \alpha(g_* - g_0)^2, \quad (14)$$

which corresponds to a Gaussian about a given gap g_0 with precision related to α . We now define the first term in (10) to regularize the future behavior of the controller, in contrast to (13) which focuses on the fit to observations. Let $\chi_{\{v \leq 0\}}(v)$ denote the characteristic function which equals zero for the real vector v having all positive components and equals infinity elsewhere. The negative log-likelihood is defined to be

$$-\log p(s_{k+1:T}^1 | s_{1:k}, s_{k+1:T}^2, \theta, \hat{\gamma}) = \beta \|a\|_{\infty} + \chi_{\{v \leq 0\}}(v), \quad (15)$$

where $a = (h(s_{k+1}, \theta), \dots, h(s_{T-1}, \theta))^{\top}$ and $v = (v_{k+1}^1, \dots, v_T^1)^{\top}$. The coefficient β determines the strength of the regularization. With the regularization terms now defined, we let $\gamma = (\alpha, g_0, \beta)$. Collecting the likelihoods specified in (13)- (15) the negative log-likelihood for a given θ in (10) is

$$\begin{aligned} f(\theta) &= \frac{1}{2\sigma_a^2} \sum_{i=1}^{k-1} (\hat{a}_i - h(s_i, \theta))^2 + \alpha(g_* - g_0)^2 + \\ &\quad + \beta \|a\|_{\infty} + \chi_{\{v \leq 0\}}(v). \end{aligned} \quad (16)$$

The σ_a^2 term contributes only to the weighting of the data fit term relative to the regularization terms. We thus may set $\sigma_a^2 = 1$ for convenience and determine the other hyperparameters relative to this.

Given parameters θ' we can obtain a predicted trajectory via the dynamics given in equation (7). This trajectory has exact probability equal to

$$\frac{\exp(-f(\theta'))}{\int_{\Theta} \exp(-f(\theta)) d\theta} \quad (17)$$

under the model. Calculating this probability directly, however, is problematic due to the large number of function evaluations used to evaluate the integral. Sampling can be used to obtain a consistent approximation, but we cannot sample θ directly from $\exp(-f(\theta))$ because it does not correspond to a distribution for which efficient samplers exist. In the next section we construct a consistent and efficient sampler for the likelihood specified by (16).

D. Efficient Sampling

Our approach to sampling from (16) has two main steps. We first solve an optimization problem to find a set of parameters $\hat{\theta}$ that has high likelihood. We then employ importance sampling to sample from (16).

1) *Importance Sampling Given $\hat{\theta}$* : We sample parameters via $\theta \sim q(\theta; \hat{\theta})$ in the higher likelihood region around $\hat{\theta}$ where q is a distribution chosen to have support over Θ and admit efficient samplers. These samples are then weighted with their importance weights

$$w = \frac{f(\theta)}{q(\theta; \hat{\theta})} \quad (18)$$

and normalized by the sum of the weights to complete the importance sampling. Since q has support over Θ the importance sampling is consistent, and depending on the choice of q this procedure may also be efficient for sampling all the high-likelihood θ . We later perform experiments to show that our choice of q yields an efficient sampler.

2) *Optimizing to Find $\hat{\theta}$* : There are multiple possible optimization problems that could be solved to find a high-likelihood $\hat{\theta}$ from $f(\theta)$. Minimizing $f(\theta)$ over $\theta \in \Theta$ directly is one choice but we see that $\forall t > k$ s_{t+1} depends on θ through both $A(\theta)$ and s_t in (7) since we only observe up to timestep k . This implies that including the future behavior regularizer terms from (15) produces a nonconvex problem. To ensure our predictions can be made in realtime we instead

Algorithm 1: Probabilistic Trajectory Prediction for Ramp Merging

Input: $s_{1:k}, s_{k+1:T}^2, \hat{\gamma}, n$
Output: $s_{k+1:T}^{1,(i)}, p^{(i)}$, for $i = 1, \dots, n$

```

1 Solve convex problem (P) for  $\hat{\theta}$ 
2 foreach  $i = 1, \dots, n$  do
3   Sample  $\theta_i \sim q(\theta; \hat{\theta})$ 
4   Generate  $s_{k+1:T}^{1,(i)}$  via (7)
5    $w_i \leftarrow \exp(-f(\theta_i, s_{1:k}, s_{k+1:T}^{1,(i)}, s_{k+1:T}^2, \hat{\gamma}))/q(\theta_i; \hat{\theta})$ 
   via (16)
6 end
7  $\forall i = 1, \dots, n \quad p^{(i)} \leftarrow w_i / \sum_{i=1}^n w_i$ 

```

optimize over all other terms in $f(\theta)$. Optimizing over the chosen terms yields

$$\hat{\theta} = \underset{\theta \in \Theta}{\operatorname{argmin}} \frac{1}{2} \sum_{i=1}^{k-1} (k_v(v_i^2 - v_i^1) + k_g(g_i - g_*) - \hat{a}_i)^2 + \alpha(g_* - g_0)^2 \quad (19)$$

$$= \underset{\theta \in \Theta}{\operatorname{argmin}} \frac{1}{2} \|D \begin{pmatrix} k_v \\ k_g \\ g_* \\ k_g g_* \end{pmatrix} - b\|_2^2 \quad (20)$$

$$= \underset{\theta \in \Theta, u \in \mathbb{R}_+}{\operatorname{argmin}} \frac{1}{2} \|D \begin{pmatrix} k_v \\ k_g \\ g_* \\ u \end{pmatrix} - b\|_2^2 \quad \text{s.t.} \quad k_g g_* = u \quad (\text{NC})$$

where we collect the variables and write the optimization as a least squares problem with the rewritten known terms being $D \in \mathbb{R}^{k,4}$ and $b \in \mathbb{R}^k$. For the last equality we use a nonconvex quadratic constraint with a dummy variable to make the vector of decision variables linear. To make this nonconvex problem amenable to methods from convex optimization we solve a semidefinite relaxation of (NC). Let $x = (\theta; u) \in \Theta \times \mathbb{R}_+$. We also rewrite the nonconvex constraint $k_g g_* = u$ in terms of x . Let

$$r(x) = x^\top E x + c^\top x = k_g g_* - u, \quad (21)$$

whereby the constraint may be written as $r(x) = 0$. By Lemma 1 in the Appendix, solving the relaxation of (NC) for x given by

$$\begin{aligned} & \underset{\substack{X \in \mathbb{S}^4 \\ x \in \Theta \times \mathbb{R}_+}}{\operatorname{minimize}} \quad \frac{1}{2} \operatorname{tr}(D^\top D X) - b^\top D x - \frac{1}{2} b^\top b \\ & \text{s.t.} \quad X \succeq x x^\top \\ & \quad \quad r(x) = 0 \end{aligned} \quad (\text{P})$$

is equivalent to solving (NC) for x . This enables us to quickly obtain $\hat{\theta}$ by solving the convex (P) rather than the nonconvex (NC). The proposed method for sampling trajectories is summarized in Algorithm 1.

IV. EXPERIMENTS

To evaluate the proposed method's ability to predict trajectories in dense traffic for ramp merging we test it on the NGSIM

dataset [9]. The NGSIM dataset includes full trajectory data recorded at 10 Hz for two highways, I-80 and US-101, during peak usage. Since our focus is ramp merging for AVs, we extract relevant pairs of lead and lag vehicles. These pairs are those between which a vehicle entering the highway has merged, or the pair behind such a pair. We are most interested in predicting the behavior of the lag vehicle at the most crucial moment—when it can see the potentially merging AV. For each pair the start of the prediction window $t = k + 1$ begins when the merging vehicle first passes the lag vehicle. The end of the prediction window $t = T$ occurs either when the vehicle passes the lead vehicle or first enters the target lane in case of a merge. All pairs are observed for at least 29 timesteps (2.9 s) before the prediction window. This choice of observation window allows us to compare to methods that use more traditional window lengths. We extract 420 pairs from the I-80 data and 292 pairs from the US-101 data.

A. Model Specifications

We place a weak prior on g_* by setting $\alpha = \frac{1}{50^2}$ and g_0 equal to the mean of the observed gaps. We fix $\beta = 15$ and $\bar{k} = 0.5$ for all experiments. For importance sampling we define $q(\theta; \hat{\theta})$ as the multivariate normal distribution $\mathcal{N}(\hat{\theta}, \operatorname{diag}(0.1^2, 0.1^2, 1))$ truncated to Θ and draw 10,000 samples.

B. Baselines

We compare to state-of-the-art methods for ramp merging and general highway prediction in addition to a simplified version of the proposed model:

- **Constant Velocity (CV):** The average velocity is used to predict future positions.
- **IDM-based (IDM)** [16] : The IDM car-following model [17] is parameterized based on the identified lead vehicle. Unlike other methods it uses the future trajectories of the lead vehicle and the potential merging vehicle.
- **Social GAN (SGAN)** [18] : Shown to achieve state-of-the-art performance on NGSIM when compared to other neural networks [7] despite originally being designed for joint prediction of pedestrian trajectories.
- **No Regularization (Proposed-NR):** The proposed method without regularization terms, corresponding to only the first term of (16).

SGAN is trained once on each highway dataset. For making predictions on a given scenario, the trained model that has not seen the scenario is used to make predictions. Unlike other methods it uses 3.2 s of observations downsampled to 2.5 Hz and makes up to 4.8 s of predictions also at 2.5 Hz.

C. Evaluation Metrics

Let $\hat{x}_{i,t}$ be the random variable corresponding to the probabilistic prediction of the vehicle's position at timestep t in the i th scenario. The true position is denoted $x_{i,t}$. Since the time horizon varies between scenarios, we denote N_t as the number of scenarios with time horizon $T \geq t$. To evaluate the

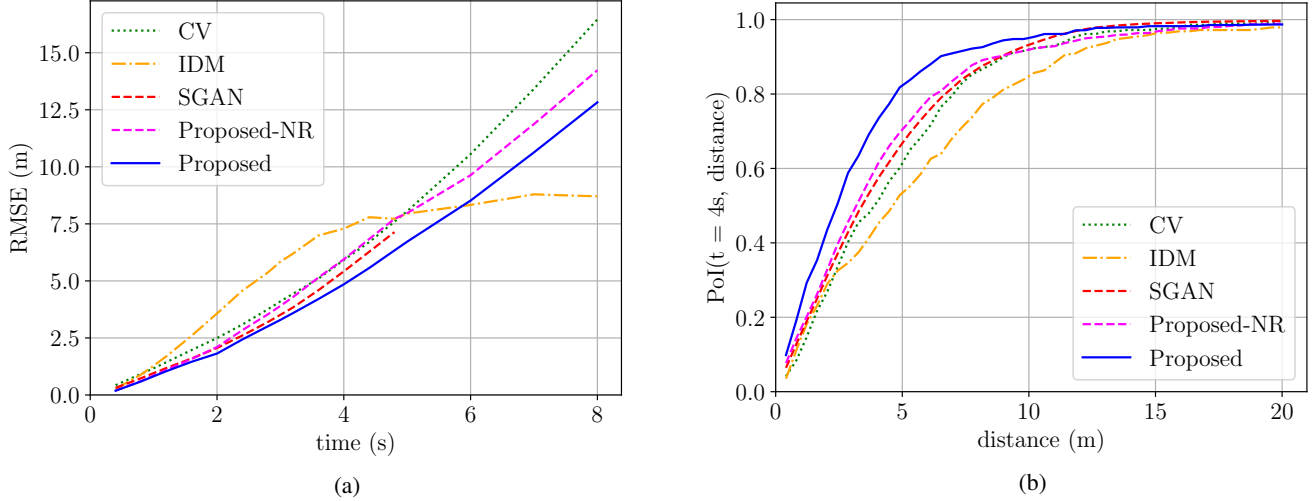


Figure 3: Predictive performance of each method on the NGSIM dataset. The RMSE in Figure 3a is evaluated at times up to 4.8 s for SGAN and to 8 s for the rest. The proposed method achieves the lowest error at almost all timesteps, while IDM achieves lower error due to it having knowledge of surrounding vehicles’ future trajectories. PoI in Figure 3b is calculated to obtain the distribution of distances of each method’s predictions at $t = 4$ from the corresponding true position. The proposed method assigns greater probability to positions closer to the true position than the other methods.

accuracy of the probabilistic trajectory predictions we evaluate the following metrics:

- *Root Mean Squared Error (RMSE)*: The square root of expected squared error between the true position and prediction, used in [4]–[7]. RMSE is calculated at timestep t as:

$$RMSE(t) = \sqrt{\frac{1}{N_t} \sum_{i=1}^{N_t} \mathbb{E}[(x_{i,t} - \hat{x}_{i,t})^2]}$$

- *Probability of Inclusion (PoI)*: For a given timestep, this is the probability that a prediction is within a given distance of the true position. This includes the minimum distance error metric in [18] as a special case and is calculated as:

$$PoI(t, d) = \frac{1}{N_t} \sum_{i=1}^{N_t} p(|x_{i,t} - \hat{x}_{i,t}| \leq d)$$

The RMSE tells us how the prediction errors are distributed on average, with more weight given to the larger errors due to the squared term within the expectation. On the other hand, calculating PoI at a fixed timestep yields the distribution of distances between the predictions and the true position of the vehicle. A prediction method could fail to make many predictions within the region around the actual vehicle, but still attain a decent RMSE by avoiding predictions far away. This behavior would be visible in the distribution given by PoI.

D. Performance in Dense Traffic Scenarios

The RMSE for each method is shown in Figure 3a. Each method has RMSE increasing over time due to the uncertainty

inherent in predicting farther into the future. The IDM method has RMSE that levels off after four seconds, but its predictions are based on knowing the future trajectories of the leading vehicles. Knowing the future trajectories of the lead vehicle and potential merging vehicle allow it to better infer possible positions of the lag vehicle. Aside from this method all others consistently outperform the constant velocity model. This better performance can be explained by their modeling of interactions between vehicles, which the constant velocity model lacks. The benefit of taking into account interactions is more pronounced for the longer-term predictions.

Figure 3a also shows the effectiveness of the regularization terms in the proposed method. Before adding these terms the method is competitive with SGAN, and the full model including the terms achieves lower RMSE at all times. The gap in performance between these methods also appears in the PoI, calculated at 4 s into the future in Figure 3b. Here the proposed method’s predictions are likely to be the closest to the true position for most distance thresholds of interest. This is shown by its curve in Figure 3b that rises more rapidly than the others. The curve for Proposed-NR also rises faster than the others for lower distances, but is surpassed by that of SGAN. This explains why SGAN achieves a lower RMSE than Proposed-NR. While SGAN makes fewer predictions with large error, leading to a lower RMSE, Proposed-NR assigns greater probability to closer predictions.

A qualitative comparison of the methods is shown in Figure 4. Here IDM effectively uses the future trajectory information to make accurate predictions. The importance of accounting for interactions is illustrated by the constant velocity model, which performs worse than the interaction-based methods during the early timesteps. Over time the predictions of all methods drift away from the true position,

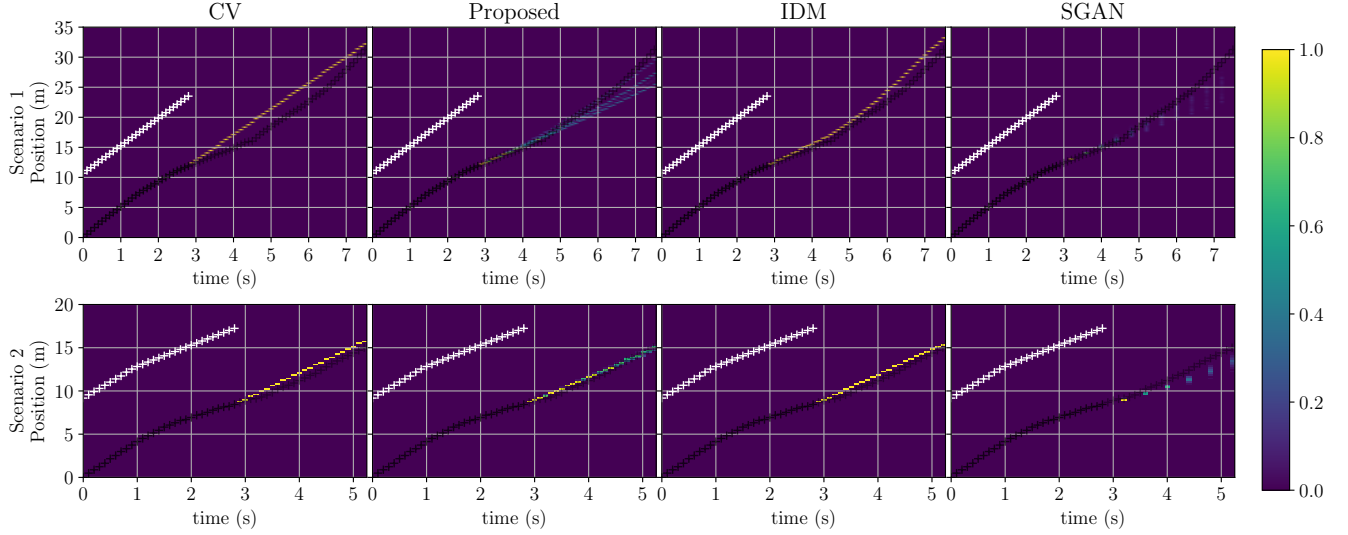


Figure 4: Predictions of each method on two ramp merging scenarios. The black crosses show the lag vehicle’s position and the white crosses show the observed positions of its lead vehicle. The probabilistic predictions for each method are displayed after the end of the observation window. The color bar (right) provides the probability corresponding to each color. The proposed method predicts the lag vehicle’s positions accurately despite using less information than the other interaction-based methods.

but some predictions made by the proposed method remain close.

E. Performance with Limited Observations

Previously we compared performance ensuring that each method had sufficiently many observations in each scenario. For the real scenarios that AVs will encounter, however, we cannot guarantee that such time will be available. Even within the NGSIM dataset alone, nearly 8% of the scenarios having at least 400 ms of observations (four timesteps) are removed from our evaluation to ensure traditional observation windows may be used. In this section we make predictions on the same scenarios as before but limit ourselves to 400 ms of observations.

To apply SGAN we fill in the initial missing observations. This is done by extrapolating from the given observations using the constant velocity model. We train the neural network on the NGSIM dataset with these extrapolated observations. The RMSE over time for SGAN and the proposed method are shown in Table I. Using fewer observations degrades the performance of SGAN. In contrast, the proposed method makes effective use of the few observations and largely maintains its original performance.

Table I: RMSE with Limited Observations. Predicting with an observation window of 400 ms instead of 3.2 s degrades the performance of both methods, but the proposed method is more robust.

Method	RMSE (meters)					
	0.8 s	1.6 s	2.4 s	3.2 s	4 s	4.8 s
SGAN	0.89	2.14	3.65	5.50	7.62	10.08
Proposed	0.55	1.33	2.33	3.58	5.10	7.02

F. Comparison of Sampling Distributions

Importance sampling allows us to obtain samples from the unnormalized density specified by (16). Depending on the choice of sampling distribution, the quality of the samples will vary. In this section we compare the sample quality of the proposed method and a sampler based on the prior distribution on θ given by $p(g_*|\hat{y})$ in (14). We define this sampler with

$$q_{\text{prior}}(\theta) = \mathcal{U}((k_v, k_g); [0, \bar{k}]^2) p(g_*|\hat{y}) \mathbb{1}\{\theta \in \Theta\} \quad (22)$$

from which we can sample (k_v, k_g) from the given uniform distribution and sample g_* from its truncated normal distribution.

For each scenario used in the NGSIM evaluation we estimate the minimum value of (16) denoted $f(\theta^*)$ and compare the distribution of the optimality gap $f(\theta_i) - f(\theta^*)$ for θ_i sampled from $q(\theta_i; \hat{\theta})$ and $q_{\text{prior}}(\theta)$. The distributions of optimality gaps averaged over all scenarios are shown in Figure 5. The much higher chance of obtaining high likelihood samples using the proposed method shows that it is more efficient than sampling from the prior distribution.

V. CONCLUSION

We propose a novel probabilistic extension for a car-following model and introduce nonconvex regularization terms to enforce realism in predicted behaviors. Through experiments we demonstrate that these terms lead to increased prediction accuracy for real scenarios in dense traffic. Comparing our model to existing methods on the NGSIM dataset shows that it achieves state-of-the-art performance. Furthermore, the proposed model maintains comparable performance when limited to using very few observations. We also demonstrate the efficiency of the proposed realtime inference procedure. In future work we plan to incorporate interactions with the merging vehicle and account for lane changes.

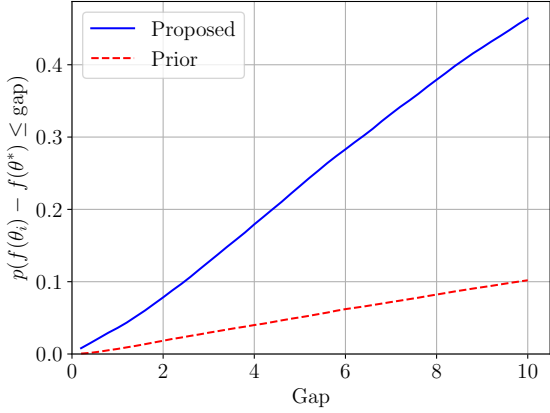


Figure 5: Cumulative distribution of optimality gaps for sampled parameters. Sampling predictions with the proposed method obtains samples of high likelihood at a higher rate than sampling from only the prior distribution on parameters.

APPENDIX

We aim to show that the original nonconvex problem given in (NC) is equivalent to the convex reformulation in (P). We first state the dual semidefinite program (SDP) of (P):

$$\begin{aligned} & \underset{s, \mu \in \mathbb{R}}{\text{maximize}} && s \\ & \text{s.t.} && \begin{pmatrix} \frac{1}{2}D^\top D + \mu B & b^\top D + \mu q \\ (b^\top D + \mu q)^\top & \frac{1}{2}b^\top b - s \end{pmatrix} \succeq 0 \end{aligned} \quad (\text{D})$$

We use the following special case of [19, Theorem 6].

Corollary 1. *Let $r : \mathbb{R}^n \rightarrow \mathbb{R}$ be defined as (21). Suppose there exist real vectors x_1, x_2 such that $r(x_1) < 0 < r(x_2)$. If the original nonconvex problem (NC) has value that is bounded below, the dual SDP (D) always has an optimal solution (s^*, μ^*) with optimal value equal to the infimum of (NC). Furthermore the infimum of (NC) is attained when the dual SDP possesses a feasible set that is not a singleton.*

Proof. This follows immediately from [19, Theorem 6]. \square

Remark 1. *Such x_1, x_2 can easily be found by taking $x_1 = (\frac{k}{2}, \frac{k}{2}, 2, 2k)$ and $x_2 = (\frac{k}{2}, \frac{k}{2}, 2, \frac{k}{2})$, yielding $r(x_1) = (\frac{k}{2})x_2 - 2k < 0 < (\frac{k}{2})x_2 = r(x_2)$.*

We now aim to show that the feasible μ are not unique to obtain equivalency.

Lemma 1. *If $D \in \mathbb{R}^{m,n}$ with $m \geq n$ as defined in (D) has full rank, then the formulations (NC) and (P) are equivalent and the optimal solution is attained.*

Proof. First note that D being full rank implies $D^\top D \succ 0$. For sufficiently small $u \in \mathbb{R}$, $\frac{1}{2}D^\top D + uI \succ 0$. For these u , $\frac{1}{2}D^\top D + \frac{u}{\|E\|_2}E \succ 0$ so the interior of $\{\mu \in \mathbb{R} : \frac{1}{2}D^\top D + \mu E \succeq 0\}$ is nonempty. Since there exist $s \in \mathbb{R}$ such that these μ are feasible for (D), and by the previous remarks, we can apply Corollary 1 to obtain the desired result. \square

REFERENCES

- [1] A. Lawitzky, D. Althoff, C. F. Passenberg, G. Tanzmeister, D. Wollherr, and M. Buss, "Interactive scene prediction for automotive applications," in *2013 IEEE Intelligent Vehicles Symposium (IV)*. IEEE, 2013, pp. 1028–1033.
- [2] S. Lefèvre, D. Vasquez, and C. Laugier, "A survey on motion prediction and risk assessment for intelligent vehicles," *ROBOMECH journal*, vol. 1, no. 1, p. 1, 2014.
- [3] B. Kim, C. M. Kang, J. Kim, S. H. Lee, C. C. Chung, and J. W. Choi, "Probabilistic vehicle trajectory prediction over occupancy grid map via recurrent neural network," in *2017 IEEE 20th International Conference on Intelligent Transportation Systems (ITSC)*. IEEE, 2017, pp. 399–404.
- [4] L. Xin, P. Wang, C.-Y. Chan, J. Chen, S. E. Li, and B. Cheng, "Intention-aware long horizon trajectory prediction of surrounding vehicles using dual lstm networks," in *2018 21st International Conference on Intelligent Transportation Systems (ITSC)*. IEEE, 2018, pp. 1441–1446.
- [5] N. Deo and M. M. Trivedi, "Convolutional social pooling for vehicle trajectory prediction," in *Proceedings of the IEEE Conference on Computer Vision and Pattern Recognition Workshops*, 2018, pp. 1468–1476.
- [6] Y. Hu, W. Zhan, and M. Tomizuka, "Probabilistic prediction of vehicle semantic intention and motion," in *2018 IEEE Intelligent Vehicles Symposium (IV)*. IEEE, 2018, pp. 307–313.
- [7] R. Chandra, U. Bhattacharya, A. Bera, and D. Manocha, "Trophic: Trajectory prediction in dense and heterogeneous traffic using weighted interactions," in *Proceedings of the IEEE Conference on Computer Vision and Pattern Recognition*, 2019, pp. 8483–8492.
- [8] J. Wei, J. M. Dolan, and B. Litkouhi, "Autonomous vehicle social behavior for highway entrance ramp management," in *2013 IEEE Intelligent Vehicles Symposium (IV)*. IEEE, 2013, pp. 201–207.
- [9] US Department of Transportation. (2008) Ngsim - next generation simulation. Accessed on: 2019-06-30. [Online]. Available: <http://www.ngsim.fhwa.dot.gov/>
- [10] J. Wiest, M. Höffken, U. Kreßel, and K. Dietmayer, "Probabilistic trajectory prediction with gaussian mixture models," in *2012 IEEE Intelligent Vehicles Symposium*. IEEE, 2012, pp. 141–146.
- [11] N. Kaempchen, K. Weiss, M. Schaefer, and K. C. Dietmayer, "Imm object tracking for high dynamic driving maneuvers," in *IEEE Intelligent Vehicles Symposium, 2004*. IEEE, 2004, pp. 825–830.
- [12] A. Houenou, P. Bonnifait, V. Cherfaoui, and W. Yao, "Vehicle trajectory prediction based on motion model and maneuver recognition," in *2013 IEEE/RSJ international conference on intelligent robots and systems*. IEEE, 2013, pp. 4363–4369.
- [13] M. Bahram, C. Hubmann, A. Lawitzky, M. Aeberhard, and D. Wollherr, "A combined model-and learning-based framework for interaction-aware maneuver prediction," *IEEE Transactions on Intelligent Transportation Systems*, vol. 17, no. 6, pp. 1538–1550, 2016.
- [14] N. Deo, A. Ranges, and M. M. Trivedi, "How would surround vehicles move? a unified framework for maneuver classification and motion prediction," *IEEE Transactions on Intelligent Vehicles*, vol. 3, no. 2, pp. 129–140, 2018.
- [15] C. Dong, J. M. Dolan, and B. Litkouhi, "Smooth behavioral estimation for ramp merging control in autonomous driving," in *2018 IEEE Intelligent Vehicles Symposium (IV)*. IEEE, 2018, pp. 1692–1697.
- [16] C. Hubmann, J. Schulz, G. Xu, D. Althoff, and C. Stiller, "A belief state planner for interactive merge maneuvers in congested traffic," in *2018 21st International Conference on Intelligent Transportation Systems (ITSC)*. IEEE, 2018, pp. 1617–1624.
- [17] M. Treiber, A. Hennecke, and D. Helbing, "Congested traffic states in empirical observations and microscopic simulations," *Physical review E*, vol. 62, no. 2, p. 1805, 2000.
- [18] A. Gupta, J. Johnson, L. Fei-Fei, S. Savarese, and A. Alahi, "Social gan: Socially acceptable trajectories with generative adversarial networks," in *Proc. IEEE Conf. Comput. Vis. Pattern Recog.*, 2018, pp. 2255–2264.
- [19] Y. Xia, S. Wang, and R.-L. Sheu, "S-lemma with equality and its applications," *Mathematical Programming*, vol. 156, no. 1-2, pp. 513–547, 2016.